Check for updates

Molecular catalyst and co-catalyst systems based on transition metal complexes for the electrochemical oxidation of alcohols

Mollie C. Morrow [ID] and Charles W. Machan [ID] *

Molecular catalysts allow deeper study of underlying mechanisms relative to heterogeneous systems by offering a discrete active site to monitor. Mechanistic study with knowledge of key intermediates subsequently enables the development of design principles through an understanding of how improved reactivity or selectivity can be achieved through modification of the catalyst structure. The co-catalytic inclusion of redox mediators (RM), which are small molecules that can aid in the transfer of protons and electrons, has been shown to improve product conversion and selectivity in many molecular systems, through intercepting key intermediates to direct reaction pathways. The primary focus for the majority of molecular electrocatalysts has been on optimizing design for reductive reactions, such as the hydrogen evolution reaction (HER), the oxygen reduction reaction (ORR), and the carbon dioxide reduction reaction (CO_2RR). By comparison, there has been much less focus on key oxidative reactions by molecular species, apart from the oxygen evolution reaction (OER). The focus of this review is to highlight molecular catalyst systems optimized for the electrochemical oxidation of alcohols. The electrochemical alcohol oxidation reaction (AOR) can serve a role in synthesizing value-added chemicals and can serve as the counterpart to the CO_2RR by releasing electricity from energy-rich molecules. State-of-the-art molecular systems for the AOR are divided between single-site catalysts and co-catalytic systems with redox mediators. The AOR is contextualized as an energy relevant reaction, an overview of the area is provided, foundational improvements in catalyst systems are highlighted, and future development principles for incorporating redox mediators are suggested.

Department of Chemistry, University of Virginia, PO Box 400319, Charlottesville, VA 22904-4319, USA. E-mail: machan@virginia.edu

Mollie C. Morrow was born in Greenwood, SC in 2000. She received her BSc from the University of South Carolina Honors College, where she worked for Prof. Aaron K. Vannucci. In 2022, Mollie began pursuing her PhD at the University of Virginia, joining the research group of Prof. Charles W. Machan. Her research focuses on the electrocatalytic oxidation of alcohols using metal complexes and redox mediators.

Mollie C. Morrow

Charles W. Machan is an Associate Professor in the Department of Chemistry at the University of Virginia, USA. He completed his BA with Majors in Chemistry and German (2008) at Washington University in St. Louis and his PhD in Chemistry (2012) under the supervision of Prof. Chad A. Mirkin at Northwestern University. Charles was a postdoctoral researcher in the laboratory of Prof. Clifford P. Kubiak from 2013–2016, before beginning his independent career at the University of Virginia. His research interests are in bioinspired and biomimetic small molecule activation, electrochemistry, and catalysis. Charles recently received the Bessel Award from the Alexander von Humboldt Stiftung.
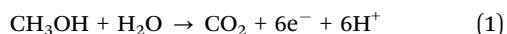
Charles W. Machan

Introduction

As the global demand for energy continues to rise, more emphasis is being given to alternative methods of energy production and reducing the demand for non-renewable energy.[1,2] The chemical industry, in particular, is both a significant consumer of energy and producer of greenhouse gas emissions.[3] There is an urgent need to revolutionize major industrial processes to reduce the corresponding impact on the terrestrial climate.[1,3] Electrocatalysis has become a cornerstone in the movement to decarbonize as it can provide an alternative synthetic route for many commodity chemicals and chemical fuels that is less energy intensive.[3,4]

Electrosynthesis starting from abundant small-molecules (*e.g.* H_2O or CO_2) to produce chemical fuels is a promising solution to address the intermittent nature of some alternative energy sources.[3] Wind and solar sources, for instance, are prone to generating energy above the demand level at peak generation times. Using this excess energy to facilitate production of chemical fuels would allow for facile storage of energy in the form of chemical bonds. The primary focus of much recent work on homogeneous systems has been on finding and optimizing electrocatalysts for key reduction reactions which produce chemical fuels, precursors, or energy, such as the hydrogen evolution reaction (HER), the oxygen reduction reaction (ORR), and the carbon dioxide reduction reaction (CO_2RR). By comparison, there has been much less focus on the key oxidative reactions which are necessary to efficiently harvest the stored chemical energy.[5] The homogeneous electrochemical alcohol oxidation reaction (AOR) mediated by transition metal complexes is understudied relative to these previous examples, despite the prevalence of AOR steps in the synthetic pathways of many commodity chemicals.[3,6]

The most widely studied oxidative electrochemical reaction is the oxygen evolution reaction (OER), which enables hydrogen production during water splitting. Hydrogen (H_2) is an ideal chemical fuel, as it releases only water as a by-product when combusted for thermal energy or decomposed in a fuel cell.[6] However, H_2 gas has several non-ideal properties, like difficulty of storage and transportation, that limit implementation.[6,7] Methanol (MeOH) is an attractive alternative fuel to due to its high energy density, surpassing H_2 at ambient conditions.[5–7] As a liquid, MeOH is more easily stored and transported at ambient temperatures and pressures in a manner compatible with current infrastructure in comparison to H_2.[5,6] MeOH is also widely available and can be easily produced from syngas or as a CO_2RR product.[5]

Direct methanol fuel cells (DMFC) utilize the methanol oxidation reaction (MOX) at the anode to generate electricity from the complete oxidation of MeOH to CO_2, which involves six electrons and six protons.[4]

$$CH_3OH + H_2O \rightarrow CO_2 + 6e^- + 6H^+ \qquad (1)$$

The mechanism by which this transformation occurs is poorly understood and assumed to be very sluggish. The reaction can be broken down into three sequential $2H^+/2e^-$ reactions, forming
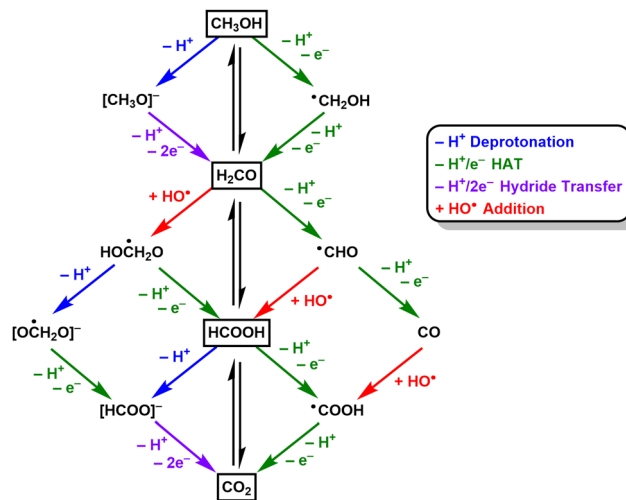

Fig. 1 Possible pathways for the oxidation of methanol to CO_2 with water present. Hydroxyl radicals are produced by the partial oxidation of water.[8]

formaldehyde and formic acid intermediates (as seen in Fig. 1) *en route* to CO_2 generation.[4,5,8] The possibility of additional reaction products produced by partial oxidation or deprotonation represents a challenge for the catalytic system, as maximizing energy density output requires selectivity for the $6H^+/6e^-$ product CO_2.[5] The most common catalysts for heterogeneous MOX in DMFCs are platinum- and ruthenium-based materials.[5] However, MOX catalysts derived from these metals still suffer from common drawbacks such as slow kinetics, large overpotentials, and poor selectivity, often leading to CO poisoning of the surface.[5,7,8]

Here, key advancements in molecular transition metal-based electrocatalyst development on MOX and AOR are highlighted. Particular emphasis is given to first-row transition metal-based systems, as much recent work in the field of homogeneous electrocatalysis has prioritized using non-platinum group metals because of the possibility for lower environmental impacts and associated cost. Heterogeneous materials for MOX have been discussed extensively elsewhere and will therefore not be covered in this work.[7] There are potential benefits to using molecular systems in the study of poorly understood reaction mechanisms. Molecular catalysts possess a discrete active site, unlike heterogeneous materials, which makes the identification and isolation of intermediates relatively easier. Mechanistic study with knowledge of key intermediates subsequently enables the development of design principles through an understanding of how improved reactivity or selectivity can be achieved through modification of the catalyst structure.[5,9] Modulation of the catalyst properties can easily be accomplished through structural modification of the active site coordination environment or substitution of metal centers. It has also been suggested in certain cases that molecular systems could provide faster reaction kinetics than their heterogeneous counterparts.[5] A strategy that has gained popularity is immobilizing molecular catalysts onto conducting supports.[7] These heterogenized catalysts are thought to combine the flexibility of molecular catalyst structure with the stability offered by

heterogeneous materials. While there have been some advancements made using this strategy, often the inclusion of a molecular anchor or a polymer binder will inherently change the properties of the catalyst; thus muddying the structure–function relationships apparent from studies under homogeneous conditions.[10,11] For this reason, we will exclude these catalysts from our review, although interested readers can find details on these systems elsewhere.[7,8,12]

A molecular catalyst system can also be improved through the inclusion of a redox mediator as a co-catalyst.[9,13] Redox mediators (RMs) aid in the transfer of protons and electrons during the reaction which can improve both the kinetics and thermodynamics of a reaction of interest (see Fig. 2).[9] RMs can assist in electron transfer between the electrode and the catalyst, or in the transfer electrons and protons between catalyst and substrate.[14] In these co-catalytic systems, often the RM allows the reaction to proceed *via* a lower energy pathway, resulting in lower overpotentials and faster rates. Structural modification of the RM can also be undertaken similarly to that of a catalyst, allowing for another opportunity to fine-tune the properties of the co-catalytic system. Despite becoming prominent for other electrochemical reactions, there are relatively few known examples of electrochemical co-catalysis for the AOR.[14–16] Here, successful strategies will be described and recommendations made for the development of other systems. Those interested in aminoxyl radicals, a well-established and ubiquitous class of metal-free homogeneous electrocatalysts for the AOR are directed to more comprehensive reviews elsewhere.[17–22] It should be noted that complementary co-catalysis strategies involving aminoxyl species and transition metals for other reactions are also known, but not within the scope of this article.[9,23,24]
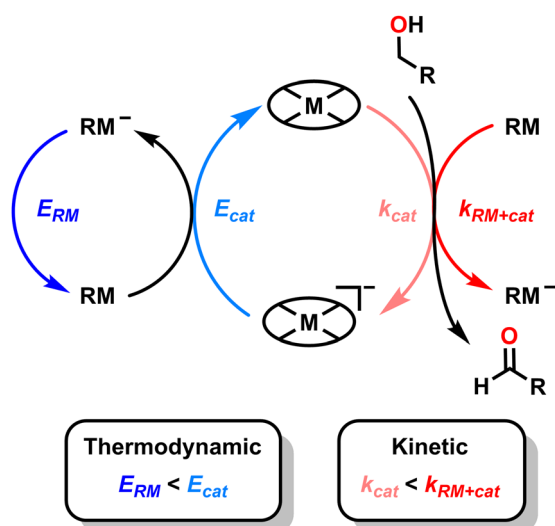

Fig. 2 Schematic depicting how inclusion of a redox mediator might benefit a molecular catalyst system kinetically (red) by increasing the rate of the reaction (k) or thermodynamic (blue) by reducing the applied potential required for catalyst regeneration (E). Proton or hydrogen atom transfers can occur either to the catalyst, the RM, or added base present under reaction conditions.

Molecular catalysts for AOR: metal-hydride intermediates

$Ni(P^R_2N^{R'}_2)$

Weiss *et al.* reported the first example of electrocatalytic AOR using a first-row transition metal in 2014.[25] They examined a family of Ni-based complexes with a diphosphene ligand framework containing pendent amine groups, P_2N_2 (1,5-R'-3,7-R-1,5-diaza-3,7-diphosphacyclooctane; R = *t*-butyl (*t*Bu); R' = phenyl (Ph), benzene (Bn), *t*-butyl (*t*Bu)). Variations of this P_2N_2 ligand framework had been employed successfully in other catalysts for electrochemical reactions, including formate and H_2 oxidation.[5,26,27] Indeed, $Ni^{II}(P^{tBu}_2N^{R'}_2)(S)_n$ (S = MeCN; n = 2, 3; R' = Ph, Bn, *t*Bu) $Ni(P_2N^{R'}_2)$ was demonstrated to be active for the AOR in the presence of a strong amine base, NEt$_3$ (pK_a(MeCN) = 18.8), using diphenylmethanol as a substrate. CV studies revealed a reversible Ni$^{II/I}$ redox feature for $Ni(P_2N^{Ph}_2)$ and $Ni(P_2N^{Bn}_2)$, but catalytic current was not observed in the presence of substrate and base.[25,26] NMR studies done using $[FeCp^{\star}_2]^+$ as a chemical oxidant indicated benzophenone was produced with a TOF of up to 114 h^{-1}, with the *t*Bu substituted catalyst $Ni(P_2N^{tBu}_2)$ achieving the greatest rate.[25]

Further work by Weiss *et al.* and Gunasekara *et al.* demonstrated that the family of $Ni(P_2N_2)$ catalysts were competent catalysts for benzyl alcohol (BnOH) oxidation, among other substrates.[28,29] $Ni(P_2N^{tBu}_2)$ CV studies show a reversible Ni$^{II/I}$ redox feature at $E_{1/2}$ = −0.76 V *vs.* Fc and the appearance of a plateau-shaped catalytic feature in the presence of BnOH and NEt$_3$ ($E_{cat/2}$ = −0.66 V *vs.* Fc).[28,29] Weiss *et al.* reported a TOF of 2.5 s^{-1} calculated from CV experiments, this was later surpassed by Gunasekara *et al.* reporting a TOF of up to 12.1 s^{-1}. CPE experiments demonstrated 90% FE for benzaldehyde (PhCHO), but the TOF was calculated to be only 6 h^{-1}.[28]

Kinetic studies revealed a complicated rate law with first-order dependence on catalyst concentration and varying dependence on substrate, base, and oxidant.[25,28,29] Hammett studies demonstrated no clear relationship between electronic effects from the substrate and TOF; however, it is noted that there are likely offsetting electronic effects at play (*e.g.* increasing electron density in the substrate may improve the favorability of alcohol coordination, but it would result in a decrease in acidity of the coordinated alcohol, making the subsequent deprotonation less favorable).[25,29] Increasing basicity of the pendent amine groups associated with different R' groups is associated with an increase in rate in oxidation.[25] However, there was no demonstrated relationship between the strength of the exogeneous base pK_a and rate.[28]

The proposed catalyst cycle for the family of $Ni(P_2N_2)$ complexes (Fig. 3) is initiated by the alcohol coordinating to the Ni^{II} metal center; this represents the rate-determining step (RDS),[30] as alcohol binding is unfavorable. Binding to the metal center weakens the O–H bond sufficiently such that alcohol ligand can be deprotonated, forming a Ni^{II}–alkoxide species. This species undergoes β-hydride elimination, resulting in the release of the aldehyde product and the formation of the Ni^{II}–H. The oxidation and deprotonation of the Ni^{II}–H species is required to
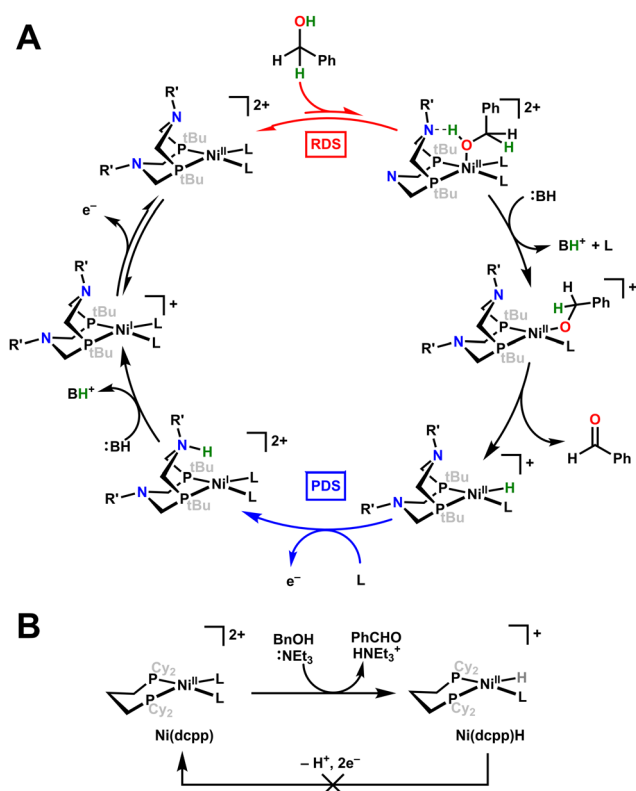
Fig. 3 (A) Catalytic cycle for **Ni(P₂N₂)** based on the most recent mechanistic study from Gunasekara *et al.* (:B = NEt₃, L = MeCN, R′ = *t*Bu, Ph, Bn) (B) Structure of Ni(dcpp) control catalyst demonstrating inaccessibility of catalyst regeneration without the pendent amine.

close the catalytic cycle. The oxidation of metal-hydrides typically require large applied potentials, but here catalysis proceeds at a modest overpotential of 0.39 V.[31] The pendent amine enables the oxidation of the metal hydride because the loss of the electron is coupled with an intramolecular proton transfer to the pendent amine, producing **Ni^I(P₂N₂(H⁺))**. This step governs the potential at which catalysis occurs and is thus defined as the potential-determining step (PDS). The re-oxidation of Ni^I is facile at this potential ($E_{1/2}$ = −0.76 V *vs.* Fc, $E_{cat/2}$ = −0.66 V *vs.* Fc).[29]

A structurally similar Ni complex without pendent amines Ni^II(dcpp)(L)₂ (dcpp = 1,2-bis(dicyclohexylphosphino)propane, L = MeCN), or **Ni(dcpp)**, is a capable stochiometric oxidant of BnOH in the presence of NEt₃ (Fig. 3B).[29] **Ni(dcpp)** is thought to operate in an analogous mechanism to **Ni(P₂N₂)** for the oxidation of BnOH, resulting in the generation of a metal-hydride intermediate. **Ni(dcpp)** ($E_{1/2}$ = −0.79 V *vs.* Fc) and **Ni(P₂N₂)** ($E_{1/2}$ = −0.76 V *vs.* Fc) both display a reversible redox feature associated with Ni^II/I at similar potentials, yet no catalytic current for **Ni(dcpp)** is observed in the presence of BnOH and base. The oxidation of **Ni(dcpp)(H)** is inaccessible (E_{app} > 0.1 V *vs.* Fc) under the studied reaction conditions, preventing any catalytic turnover.[29] The crucial difference between **Ni(dcpp)** and **Ni(P₂N₂)** is the presence of the pendent amine, which is attributed to why **Ni(P₂N₂)(H)** is oxidized at such a mild

potential ($E_{cat/2}$ = −0.66 V *vs.* Fc). Examining the behavior of **Ni(dcpp)** lead to two important conclusions: (1) the pendent amine is not necessary for BnOH oxidation but (2) the pendent amine does facilitate the oxidation of the M–H.[29]

In addition to the evidence presented in the **Ni(dcpp)** system, DFT studies indicate that the pendent amine is not basic enough (conjugate acid pK_a(MeCN) = 6–9) to deprotonate the BnOH ligand (pK_a(MeCN) = 13–17); thus deprotonation by the exogeneous base, NEt₃ (conjugate acid pK_a(MeCN) = 18.8) is the favorable pathway.[29] Rather than deprotonating the BnOH, the pendent amine likely stabilizes the species *via* hydrogen bonding between the H of the alcohol and N of the pendent amine.[29] The crucial role of the pendent amine is facilitating the oxidation and deprotonation of the Ni^II–H species. The exact mechanism by which the pendent amine aids in the oxidation of **Ni(P₂N₂)(H)** has not been examined, but Gunasekara *et al.* speculated that there is an intramolecular proton transfer from the Ni to the pendent amine as part of a PCET step. This assumption is based on (1) the relative kinetic favorability of an intramolecular PCET reaction over a bimolecular PCET reaction and (2) that others have reported similar reductions in overpotential with systems that bypass the direct oxidation/deprotonation of metal-hydride intermediates.[15] A sequential mechanism was dismissed (PT–ET or ET–PT) based on the work of Hammes–Schiffer and co-workers demonstrating that a concerted mechanism is favored for an analogous intramolecular oxidation/deprotonation step using a similar Ni catalyst with P₂N₂ ligands.[32,33]

Computational studies by Gunasekara *et al.* identified an off-cycle high-spin **Ni(P₂N₂)(BnOH)(L)₃** species resulting from the coordination of an additional L ligand (likely MeCN) that inhibits catalytic TOF by a factor of 8.[29] It is likely that the most favorable configuration for **Ni(P₂N₂)** is the axial binding of the alcohol ligand, but once deprotonated, the alkoxide ligand is more stable in an equatorial position complicating the mechanism with an additional isomerization step. The **Ni(P₂N₂)** species also demonstrated an affinity for binding amine bases, which is also thought to have an inhibitory effect on catalysis.[28,29] Controlling the accessibility of variable ligand coordination modes might therefore be an avenue to explore to improve catalysis by disfavoring off-cycle intermediates. Although the inclusion of additional pendent bases through the use of a P₂N₂ ligand was thought to be a beneficial strategy, the coordination of two P₂N₂ ligands was found to inhibit AOR.[25] Shifting the equilibria of one or more labile solvent species through the inclusion of stronger field ligands may inhibit the formation of competitive high-spin species, but any structural modification comes with inherent changes to electrochemical behavior.[29]

To date, the **Ni(P₂N₂)** family demonstrates one of the more active systems for AOR without requiring prohibitively large overpotential or strong bases. The substrate scope is one of the most robust, including isopropyl alcohol (IPA), ethanol (EtOH), other secondary aliphatic alcohols, and substituted benzyl alcohols. Data on product selectivity is incomplete and should be evaluated in future studies. Unfortunately, **Ni(P₂N₂)** has yet

to successfully be employed for MeOH. Previous attempts showed signs that MeOH may actually be leading to catalyst decomposition.[28] Overall, the **Ni(P$_2$N$_2$)** system is a good example of the benefits that metal–ligand cooperativity (MLC) can provide by facilitating intramolecular reactions.

(Fe)(PNP)

McLoughlin *et al.* published another example of first-row transition metal based electrocatalyst for AOR in 2020.[34] The Waymouth group previously demonstrated the successful adaptation of a thermal catalyst used for transfer hydrogenation (TH) reactions for the electrocatalytic AOR.[35] In 2020 they demonstrated that an Fe-based thermal catalyst for acceptorless alcohol dehydrogenation (AAD) could be successfully adapted for the AOR utilizing IPA as a substrate and a phosphine base.[34,36,37] The overall AAD mechanism requires a thermal AOR step, which, provided the AAD catalyst operates at room temperatures, makes it a viable strategy for developing new electrocatalyst systems.[36,38] The authors targeted an Fe-pincer compound Fe^{II}(PNP)(CO)(H) (PNP = bis[2(diisopropylphosphino)ethyl]amine), or **FeN** as a suitable species for adaptation to the AOR.[39] NMR studies confirm that **FeN** indeed oxidizes IPA to form acetone, generating a key intermediate, **Fe(H)(NH)**, in the process (see Fig. 4(A)). CV and DFT studies demonstrate that **Fe(H)(NH)** is then able to be oxidized and deprotonated at mild potentials, albeit with strong base (P$_2$-Et, conjugate acid pK_a(THF) = 25.3), to reform **FeN**.

The Fe-pincer compounds having well-studied behavior for AAD was essential to identifying it as a suitable electrocatalyst candidate and for understanding finer mechanistic details to optimize the electrocatalytic response.[34,40] Previous work with **FeN** as a AAD catalyst would indicate that IPA coordinates in a *syn* manner (see Fig. 4(B)) through H-bonding to the Fe metal center and the N on the PNP ligand.[41] This facilitates the possible formation of a six-membered transition state, where ultimately both a net 2H$^+$/2e$^-$ transfer occurs to the Fe complex and acetone is released.[34,41] This part of the mechanism is

facile and occurs at room temperature with no added base. In CV studies, upon addition of IPA to **FeN**, a new oxidation peak appeared at −0.74 V *vs.* Fc, associated with the Fe$^{III/II}$ redox process of the **Fe(H)(NH)** generated *in situ*. The oxidation of **Fe(H)(NH)** is irreversible as observed by CV (*E* = −0.74 V *vs.* Fc), indicating it is followed by a fast chemical step. Upon undergoing a 1e$^-$ oxidation [**Fe^{III}(N)(NH)**]$^+$ would be formed, an unstable radical species which is anticipated to quickly react. In the presence of IPA and sufficient base (P$_2$-Et, conjugate acid pK_a(THF) = 25.3), catalytic current enhancement is observed (*E*$_{cat}$ = *ca.* −0.65 V *vs.* Fc). The onset potential coincides with the *E*$_{ox}$ of **Fe(H)(NH)**, indicating that is the PDS for this reaction.

The **Fe(H)(NH)** intermediate is then proposed to undergo a 2H$^+$/2e$^-$ oxidation and deprotonation to regenerate **FeN** and close the catalytic cycle. The proposed mechanism by which this occurs was further illuminated by DFT studies, which supported the initial 1e$^-$ oxidation to [**Fe^{III}(H)(NH)**]$^+$. Theory suggested that the metal center proton would be deprotonated first, as the pK_a of the Fe–H bond was calculated to be 12.7, compared to a pK_a of 16.2 for the N–H bond. Despite this relatively mild calculated pK_a, no catalysis was observed with bases weaker than P$_2$-Et, even up to those with a conjugate acid pK_a of 21. The additional driving force required by the strong base was proposed to signify that this deprotonation is the RDS. Following this, the oxidation and subsequent deprotonation by a second equivalent of base should both be facile, since the calculated oxidation potential is lower than the applied potential during catalysis and the N–H is estimated to be a stronger acid in the oxidized species [**Fe^{II}(NH)**]$^+$ (calc. pK_a = 10.8). The final mechanistic assignment for the regeneration of **FeN** from **Fe(H)(NH)** is *via* an ECEC pathway, although the possibility of concerted pathways was not discussed.

Overall, this system displayed decent activity for the 2H$^+$/2e$^-$ oxidation of IPA to acetone, though with a substantial overpotential of 1.1 V.[31] A TOF of 1.9 s^{-1} was calculated *via* CV methods, though the authors note this analysis is not designed to be used with irreversible redox features as observed here.[34,42] They report a TON of 1.9 from CPE (*E*$_{app}$ = −0.80 V, ∼4 h), which is likely more representative of the true activity of the system. The authors attribute the low TON to catalyst decomposition over time, which is confirmed by experimental data demonstrating that under CPE conditions the **Fe(H)(NH)** species decomposes. Decomposition is thought to be the result of isomerization, resulting in the subsequent formation of an inactive neutral Fe species and free ligand.[34,40] Interestingly, this is also reminiscent of the off-cycle species inhibitory species observed with the **Ni(P$_2$N$_2$)** catalysts and described above.[29] Despite these woes, the selectivity for acetone is quantitative, suggesting that modifications to improve stability under electrolysis conditions will be beneficial.

Co(P$_3$)

Seeking to continue expanding the scope of first-row transition metal catalysts for the AOR, Heins *et al.* published the first molecular cobalt catalyst featuring a tridentate phenylphosphine ligand. Co^{II}(P$_3$)(S)$_2$ (P$_3$ = bis(2-diphenylphosphinoethyl)-phenylphosphine, S = CH$_3$CN) or **Co(P$_3$)** was demonstrated to

Fig. 4 (A) Catalytic cycle of Fe-pincer complex, **FeN**, proposed in McLoughlin *et al.* (R = iPr$_2$, :B = P$_2$-Et). (B) Six-membered transition state involving a 2H$^+$/2e$^-$ transfer between acetone to the metal center and PNP ligand.

be a stochiometric oxidant of benzyl alcohol to benzaldehyde with a sufficiently strong base, forming 2 equiv. of the oxidized **Co^I(P$_3$)** catalyst in the process. Under electrochemical conditions, **Co(P$_3$)** can be regenerated by a 1e$^-$ oxidation from **Co^I(P$_3$)** ($E_{1/2}$ = -0.78 V vs. Fc). Under electrocatalytic CV conditions, the authors reported no current enhancement associated with catalysis indicating the reaction is happening too slowly for observation on the CV timescale (<0.1 s^{-1}). Assuming the Co$^{II/I}$ redox potential would govern catalysis, they ran their CPE experiments at a sufficiently positive potential (E_{app} = -0.63 V vs. Fc) and indeed PhCHO was detected. The system was stable for 2.25 h and 97% selective for PhCHO production. While the calculated TON is an impressive 19.3, the TOF is estimated to be <0.1 s^{-1} due to the lack of observable catalysis by CV (the authors do not report a TOF calculated from CPE).[43] It is however noteworthy that the estimated overpotential is one of the lowest reported at ca. 0.2 V.[31]

Kinetic studies using [FeCp*$_2$]$^+$ as a chemical oxidant, along with DFT calculations, were used to supplement their mechanistic investigations in lieu of CV studies. Saturation kinetics were observed for [alcohol], indicating that catalysis is initiated by pre-equilibrium alcohol binding to the Co^{II} metal center. This step is necessary as iPr$_2$EtN (conjugate acid pK$_a$(MeCN) = 18.8) is not capable of deprotonating free benzyl alcohol (O–H pK$_a$(MeCN) = ca. 28), but instead requires the increase in effective acidity associated with the alcohol binding to the Co center. Indeed, DFT studies indicate that the bound alcohol should have a much lower O–H pK$_a$(MeCN) of ~12–17. Following deprotonation, the resultant **Co(P$_3$)**–alkoxide adduct is proposed to undergo a β-hydride elimination, releasing PhCHO and forming **Co(P$_3$)(H)**. Unlike other catalysts described in this Perspective, the metal-hydride intermediate does not represent the apparent limiting part of this mechanism: regeneration of **Co(P$_3$)** is facile following an ECE mechanism.

From the **Co(P$_3$)** system, it is possible to extract some design principles: alcohol coordination or metal-alkoxide formation to the catalyst should ideally be energetically favorable. While the overall reaction (ΔG° = -17.7 kcal mol^{-1}) is thermodynamically favorable, formation of the alcohol-coordinated species is uphill by between 9–14 kcal mol^{-1}. Catalyst degradation also posed a problem in this system; during CPE the current decayed in less than 3 hours. It was found in control experiments that **Co(P$_3$)** decomposes over time when exposed to iPr$_2$EtN, which likely contributed to the significant catalyst decomposition observed in post-electrolysis studies. Thus, catalyst compatibility with the reaction conditions could be addressed in future studies by identifying a more suitable base.

Molecular catalysts for AOR: metal–oxo intermediates

Fe(TAML)

A recent example of a metal-oxo catalyst was reported by Das et al. in 2019, using an iron-based electrocatalyst for the AOR supported by a tetraamido macrocyclic ligand (TAML) framework, **Fe(TAML)**.[44] Unlike the examples described to this point, this complex requires the inclusion of water as a co-substrate to produce high-valent oxo species prior to substrate oxidation, and metal hydrides are not implicated as intermediates. Another unique aspect of the reported **Fe(TAML)** system is that it operates in mixed aqueous/organic conditions without the presence of a strong base, instead relying on a buffer (pH 6–9). High-valent metal-oxo complexes have frequently been employed as synthetic oxidants due to their highly reactive nature.[45–48] Other **Fe(TAML)**-based complexes have also been employed for other oxidative chemical transformations, including for the electrochemical OER.[49,50] The oxo intermediates are powerful oxidants: Das et al. also found that the compound could electrocatalytically activate C–H bonds, consistent with its known thermal reactivity.

Das et al. found that the high-valent metal-oxo species **Fe^V(TAML)(O)** can be generated in situ from the commercially available **Fe^{III}(TAML)(OH$_2$)** at sufficiently positive applied potentials (Fig. 5). This happens via sequential PCET reactions at the electrode in the presence of a suitable base (2H$^+$/2e$^-$ removed overall). **Fe^V(TAML)(O)** was determined to be the active catalytic species through CV and CPE experiments; though the off-cycle bridged-oxo dimer species, **(Fe^{IV})$_2$(μ-O)**, has also been known to act as an electrocatalyst.[44,51] Kuiry et al. further probed the **Fe(TAML)** mechanism in a later study and found that BnOH oxidation involves a net hydride transfer (2H$^+$/1e$^-$) consisting of a HAT reaction from BnOH to the Fe-oxo intermediate, followed by a 1e$^-$ oxidation of the benzyl radical to generate the aldehyde.[51] Hammett studies revealed that the catalyst reacts preferentially with electron-rich substrates, supporting the proposal that cleaving the α-CH bond in BnOH is the RDS for this mechanism. This mechanistic proposal is also supported by a measured KIE of 1.8 using a BnOH substrate deuterated at only the α-C position.

The reported **Fe(TAML)** systems have a varied substrate scope, including many benzylic and secondary alcohols. However, since a formally Fe^V-oxo species is required, the applied electrolysis potential (E_{app} = 0.77 V vs. Fc) is positive of many of the other examples described here. While the conversion and yields for their electro-synthetic reactions are impressive (BnOH 97% conversion; PhCHO 93% yield), the Faradaic
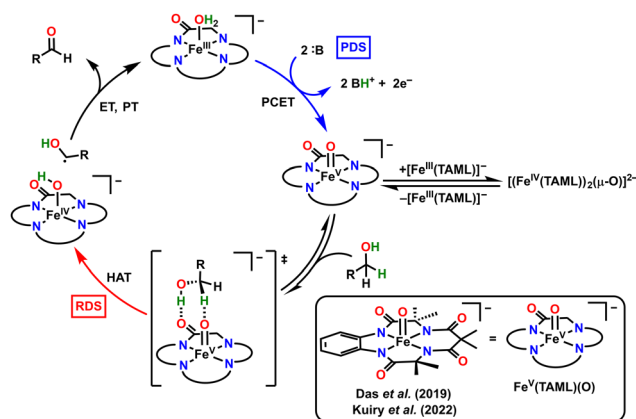

Fig. 5 **Fe(TAML)** proposed catalytic cycle of electrochemical AOR based on the work by Das et al. and Kuiry et al. (:B = phosphate buffer pH 6–9).

efficiencies are poor ($\sim 29\%$). The authors attribute this low efficiency to the competing OER, for which these compounds are also competent catalysts.[44,51]

Interestingly, the **Fe(TAML)** system has many parallels with previous work done on its heavier analogue, Ru, which can also be oxidized electrochemically to catalytically competent oxo compounds.[27,52–54] In 1980, Moyer *et al.* demonstrated that $[Ru^{IV}(bpy)(tpy)(O)]^{2+}$ (bpy = 2,2'-bipyridine, tpy = 2,2',2''-terpyridine), $[\mathbf{Ru(tpy)(bpy)(O)}]^{2+}$ could be electrochemically generated in an aqueous solution from $[\mathbf{Ru^{II}(tpy)(bpy)(OH_2)}]^{2+}$.[55] This system demonstrated a wide substrate scope for oxidation, including alcohols, aldehydes, hydrocarbons and olefins. **Ru(tpy)-(bpy)(O)** is a strong enough oxidant that only a mild aqueous buffer (pH 7–9) was required to access catalytic behavior. Interestingly, **Ru(tpy)(bpy)(O)** was also capable of oxidizing substrates beyond the $2H^+/2e^-$ product directly to up to $12e^-$ in the oxidation of *p*-xylene to terephthalate without accumulating intermediates.[55] This is in contrast to how we typically conceptualize the AOR as being bottlenecked in $2H^+/2e^-$ transformations step-by-step, as introduced above when considering MeOH conversion to CO_2.

Both the **Fe(TAML)** and **Ru(tpy)(bpy)** systems required high oxidation states in the active species; one possible way to ease this electronic burden is to have a catalyst structure over which oxidizing equivalents can delocalize. One class of compounds with excelled charge delocalization properties are those of the tri-ruthenium oxo-centered cluster, $[Ru_3(\mu_3\text{-}O)(\mu\text{-}OAc)_6(L)_3]$ (OAc = CH_3COO^-).[56–58] Clusters of this type have previously been explored as electrocatalysts, in part due to the unique charge delocalization across the three Ru centers *via* the central oxo ligand.[57,59–62] This charge delocalization enables the Ru sites in the cluster to become a competent oxidants at lower formal oxidation states compared to some mononuclear catalysts, such as the Fe^V oxidation state described above for the key $[\mathbf{Fe(TAML)(O)}]^-$ intermediate.[57,59,62] Derivatives of this oxo-centered cluster have been explored as electrocatalysts for AOR by the Toma group.[59,62] Notably, they have demonstrated $Ru_3O(OAc)_6(py)_2(L)$ (L = MeOH, H_2O; py = pyridine), **Ru₃O**, to be a competent electrocatalyst for the oxidation of BnOH in aqueous solutions.[62] Under aqueous conditions, an intermediate Ru-oxo species is proposed, similar to both the **Fe(TAML)** system and the mononuclear Ru species of Meyer and co-workers.[54,55] Under buffered conditions, two protons and two electrons can be removed overall from the cluster, producing a cationic Ru-oxo species, $[\mathbf{Ru_3^{IV,IV,III}(O)}]^+$, where the formal oxidation states for all three Ru centers are indicated. Although not experimentally quantified, it is assumed that this Ru-oxo species activates the BnOH substrate *via* a similar mechanism to that described for $[\mathbf{Fe(TAML)(O)}]^-$ and $[\mathbf{Ru(tpy)(bpy)(O)}]^{2+}$, generating a $[\mathbf{Ru_3^{III,III,III}(OH_2)}]^+$ species to close the catalytic cycle.

Uniquely among the mononuclear catalyst systems described here, activity for MeOH oxidation was reported in a subsequent publication by Toma and co-workers.[59] Unlike the BnOH oxidation in aqueous conditions, MeOH was used as solvent and substrate, implying that alcohol coordination and deprotonation occurs prior to oxidation. However, metal hydride intermediates were not directly verified: it was proposed that the two electron transfers to the cluster are accompanied by successive deprotonation reactions by the exogenous base (sodium trifluoroacetate). Given the steric hindrance at the sole active Ru site, this is a reasonable possibility, but further mechanistic testing and direct preparation of the Ru hydride intermediate would be beneficial. Further, given the behavior of the other systems with oxo intermediates, it is also still possible that adventitious water results in the formation of oxo species as the key intermediate, which could be elucidated spectroelectrochemically. Since a relatively weak base is used, the required potentials are significantly positive, however, catalytic activity for MeOH oxidation is rare for molecular systems.

AOR using redox mediators

Cu/TEMPO

The first demonstration of a co-catalyst system[9] for the electrocatalytic AOR was reported in 2016 by Badalyan and Stahl, in which they combine TEMPO (2,2,6,6-tetramethyl-1-piperidine *N*-oxyl), a known AOR catalyst, with a Cu^{II} co-catalyst.[14] This combined system was known to function thermally with O_2 as the terminal oxidant;[63–65] Badalyan and Stahl substituted the applied potential of an electrochemical cell for O_2, enabling the electrochemical AOR. Notably, in the co-electrocatalytic system, TEMPO is proposed to function as a redox mediator (RM), as opposed to a catalyst. TEMPO is a stable radical species, which after undergoing a $1e^-$ oxidation ($E = 0.24$ V *vs.* Fc), forms TEMPO$^+$, a powerful catalytic oxidant when combined with an appropriate base. The use of TEMPO, and other nitroxyl species, as both a thermally and electrochemically driven alcohol oxidation catalyst, is well studied.[18,20,22,26,63,65–68] When used as the sole catalyst for the electro-oxidation of an alcohol, TEMPO$^+$ undergoes a $1H^+/2e^-$ reduction by the alcohol substrate to form TEMPOH and the corresponding aldehyde product in the presence of a base. TEMPOH must then be re-oxidized and deprotonated ($1H^+/2e^-$) to form the active species TEMPO$^+$ for the catalytic cycle to continue. The re-oxidation to form the active TEMPO$^+$ species is limited by the highly oxidizing electrode potential required, which also leads to catalyst degradation.[14]

The cooperative **Cu/TEMPO** system conveniently side-steps the need for highly oxidizing potentials by utilizing (bpy)-$Cu^{II}(OTf)_2$ (bpy = 2,2'-bipyridine, OTf = trifluoromethanesulfonate), Cu^{II}, to mediate the oxidation of TEMPOH to TEMPO in the presence of a Brønsted base acting as a proton acceptor (See Fig. 6). The resulting Cu^I species can then be easily oxidized back to Cu^{II} at the anode of the electrochemical cell ($E = -0.18$ V *vs.* Fc). The authors found that the onset of catalysis ($E_{cat} = -0.14$ V *vs.* Fc) occurs at the $Cu^{II/I}$ redox couple under co-catalytic conditions. Thus, Cu^{II} also serves to cooperatively activate the alcohol substrate by initially forming a Cu^{II}-alkoxide adduct, which then allows TEMPO to serve as a hydrogen atom transfer (HAT) mediator during the formation
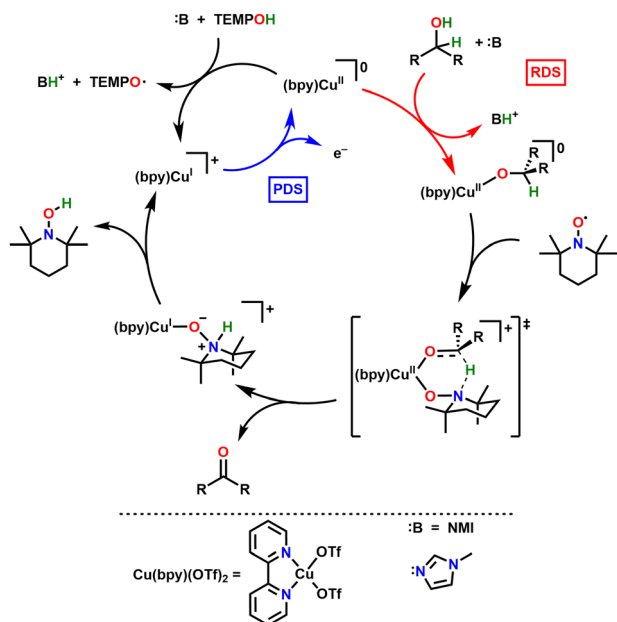
Fig. 6 Cu/TEMPO co-catalytic cycle based on that proposed by Badalyan and Stahl.[31]

of the benzaldehyde product. By eliminating the need to form the TEMPO$^+$ species, the **Cu/TEMPO** system reduced the oxidation potential of BnOH from 0.36 V *vs.* Fc (TEMPO only) to −0.14 V *vs.* Fc. The co-catalytic system also demonstrated a remarkable improvement in TOF from 2.3 s^{-1} to 11.6 s^{-1} as determined from CV experiments.

After forming the **Cu^{II}**–alkoxide adduct, which is proposed to be the RDS based on mechanistic experiments, the **Cu/TEMPO** system is thought to proceed through a six-membered transition state with TEMPO coordinating (through the O-atom) to the **Cu^{II}**–alkoxide species.[64,65] Although the next reaction of this step is a net hydride transfer, this can be divided between concerted HAT between the alkoxide to the N-atom on TEMPO, concomitant with a 1e$^-$ reduction of the **Cu^{II}** metal center to **Cu^I**. Notably, this system avoids the formation of a metal-hydride intermediate, which often leads to competing HER.[15]

Rodrigues *et al.* recently investigated how the speciation of the Cu co-catalyst might be improved upon by including additional chelating ligands.[69] Rodrigues *et al.* discovered that as the number of coordinated bpy ligands increased, the **Cu$^{I/II}$** $E_{1/2}$ decreased, indicating the bpy ligands provide additional stabilization to the **Cu^I** species, likely through strong pi-backbonding. This finding was supported by DFT calculations of ΔG values, which mirrored the experimental CV data. Under catalytic conditions (BnOH, NEt$_3$) the Cu(bpy)$_2$ species had the greatest current increase along with the least positive onset potential. Additional equivalents of ligand beyond two was found to inhibit catalytic current, despite having a more favorable $E_{1/2}$, as the dissociation of a bpy would be required in order to allow BnOH and TEMPO to bind to the active site. It should be noted, however, that TOF and FE metrics were not included and could vary from the original system.

Ru/Ru

McLoughlin *et al.* noted the prevalence of metal-hydride intermediates in other molecular electrocatalytic AOR systems; often the prohibitive step in regeneration of the catalyst due to the sluggish kinetics of the stepwise proton and electron transfer processes. Similarly to the work of Badalyan and Stahl, this work also drew inspiration from a thermal system. [Ru(CNN)-(dppb)(X)] (CNN = 2-aminomethyl-6-tolylpyridine, dppb = 1,4-bis(diphenylphosphino)butane, X = Cl or H) was previously demonstrated to be a successful catalyst for the transfer hydrogenation of ketones, producing acetone from IPA to provide the reducing equivalents for the reduction of other ketones.[35] As an electrocatalyst, Ru(CNN)(dppb)(X) was found to be active for the AOR using an alkoxide base and sufficiently positive potentials. Mechanistic study determined the metal hydride Ru^{II}(CNN)-(dppb)(H), or **RuH**, formed in the catalytic cycle after release of acetone to be a crucial intermediate (see Fig. 7). It is the 2H$^+$/1e$^-$ oxidation of the metal hydride species that is proposed to be both the RDS and the PDS ($E_{1/2}$ = −0.8 V *vs.* Fc).[15,35] **RuH** is an impressive catalyst in its own right with a TOF of 4.8 s^{-1} found using CV and an FE of 94 ± 5% found from CPE (E_{app} = −0.6 V *vs.* Fc).[35]

McLoughlin *et. al* sought to improve upon the system by finding a suitable RM to facilitate the oxidation of **RuH**.[15] Stepwise proton and electron transfer reactions often have high kinetic barriers, leading to a sluggish turnover when part of a catalytic cycle, while a concerted HAT should proceed more rapidly.[15,70] The authors reasoned that a known HAT acceptor could be integrated into the catalytic cycle by facilitating the turnover of the catalyst back to an active species without needing to apply a large overpotential.

To narrow the criteria in searching for a suitable HAT acceptor as a RM, McLoughlin *et al.* proposed the following guidelines they used for their search: (1) the BDFE of the formed RM–H bond must be similar to the BDFE of the M–H, (2) the $E_{1/2}$ and pK_a of the RM must be close to the thermodynamic potential for the AOR, (3) the $E_{1/2}$ of the RM should be oxidized at a lower potential than the M–H, and (4) the pK_a of the RM or any other components should not be able to protonate the M–H or promote HER. Following these guidelines should ensure that the desired HAT regeneration reaction is the kinetically and thermodynamically favored pathway.

They specifically targeted a transition metal complex as their HAT acceptor because the relevant thermodynamic properties ($E_{1/2}$ and pK_a) can be modulated by changing the ligand framework or metal center.[15] A suitable RM was identified in [Ru^{III}(acac)$_2$(pyimN)] (acac = 2,4-pentanedionato, pyimN = 2-(2′-pyridyl)imidazolyl) or **Ru$_{RM}$N**, which was previously identified as a HAT acceptor using the redox-active pyimN ligand.[15,71] **Ru$_{RM}$N** was chosen by the criteria set out prior: it is a capable H-atom acceptor from donors with BDFE ≤62 kcal mol^{-1} (in MeCN), the subsequently formed **Ru$^{II}_{RM}$NH** is deprotonated (pK_a(MeCN) = 22.1) and oxidized ($E_{1/2}$ = −1.00 V *vs.* Fc in MeCN) under conditions which neither protonate the catalyst **RuH** nor promote HER in the presence of the desired substrates.[15,71] Indeed, addition of the RM lowered the oxidation potential of
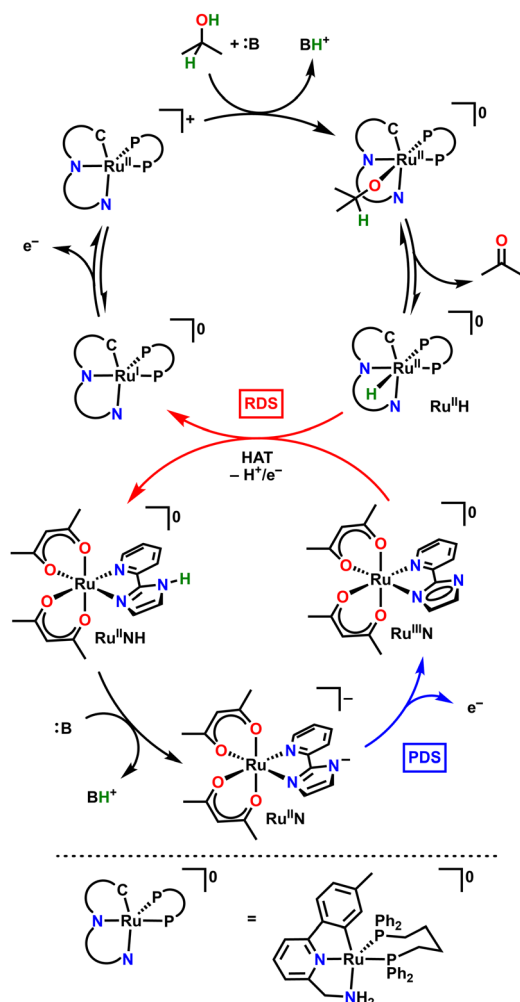
Fig. 7 Ru/Ru co-catalytic cycle proposed by McLoughlin *et al.*[15] (:B = KO*t*Bu, P$_4$-*t*Bu).

Fig. 8 (A) Ir/PhO co-catalytic cycle proposed by Galvin and Waymouth (R = iPr$_2$, :B = P$_2$-Et) adapted[31] and (B) phenol derivate mediators tested as redox mediators.

IPA by **RuN** from −0.85 V to −1.30 V *vs.* Fc; a 450 mV decrease in operating potential. They report a modest faradaic efficiency of 85% for acetone but note that acetone production at the same potential without the RM present is functionally zero, demonstrating the remarkable reduction in operating potential under co-catalytic conditions. Interestingly, the authors report a decrease in TOF by 50–75% upon inclusion of the RM. They do not speculate as to the cause for the decrease but note prior that introducing a RM to the catalyst system does increase the kinetic complexity of the reaction.

Ir/Phen

Galvin and Waymouth published another co-catalytic system around the same time as McLoughlin *et al.* which goes about tackling the metal-hydride in a similar manner, aiming to sidestep the sequential ET and PT reactions by implementing HAT reactions to facilitate the oxidation of a metal-hydride intermediate.[16] Based on prior work identifying transfer hydrogenation catalysts and acceptorless alcohol oxidation catalysts as good candidates for electrocatalytic AOR,[15,34,35] they chose
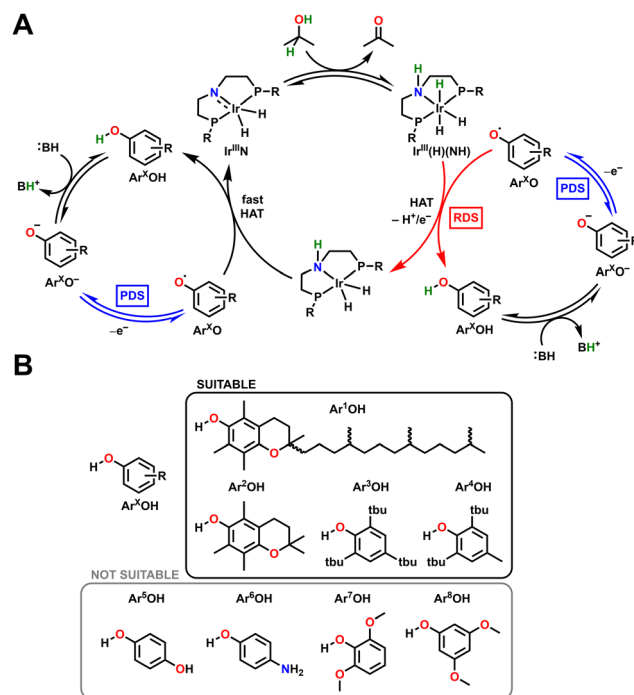
[(PNP)Ir^{III}(H)$_2$] (PNP = (bis[2-diisopropylposphino)ethyl]amide), or **IrN**, as their electrocatalyst (see Fig. 8(A)).[72] **Ir(H)(NH)** is readily formed in the excess of IPA with **IrN** (where the amide in the PNP ligand is not protonated). **IrN** was previously identified as a transfer hydrogenation catalyst capable of producing acetone from IPA.[73] The authors identified **IrN** as a suitable target electrocatalyst for the AOR based on the following guidelines: (1) the catalyst must rapidly dehydrogenate alcohols, (2) it must tolerate electrochemical conditions, and (3) be susceptible to oxidation by HAT. Indeed, **IrN** is capable of electrocatalytic AOR with a sufficiently strong base, producing acetone from IPA with moderate operating potential (E_{cat} = −0.65 V *vs.* Fc) and decent selectivity (78%, E_{app} = −0.335 V *vs.* Fc).[16] The authors then set out to identify a suitable redox mediator, noting the importance of the RM being a strong H-atom acceptor and sufficiently acidic such that the same base used in the unmediated catalysis can deprotonate it. Additionally, they highlight that the RM should be electrochemically regenerable at a less positive potential than where unmediated catalysis by **IrN** intrinsically occurs.

They identified phenoxy radical compounds as a suitable target group, which can easily be accessed by the deprotonation of the corresponding phenol and subsequent 1e$^-$ oxidation to form the phenoxy radical.[74] The thermodynamic properties of the parent phenol can be altered by inclusion of functional groups on the aromatic backbone, allowing for fine-tuning of pK_a and $E_{1/2}$. Regardless of structural modification, most phenols have a BDFE in excess of 73 kcal mol^{-1}; thus they are capable of abstracting a H-atom from most any metal-hydride, whose BDFEs generally fall around 45 to 60 kcal mol^{-1}.[74]

Galvin and Waymouth then examined a series of phenol derivates, **Ar^{x}OH**, which undergo a $1H^+/1e^-$ oxidation to form the phenoxyl radical mediators, **Ar^{X}O**, using P$_2$-Et (conjugate acid pK_a(THF) = 25.3) as a base (see Fig. 8(B)). Inclusion of α-rac-tocopherol (**Ar^{1}OH**) with **IrN** and IPA resulted in a reduction of operational potential by almost 400 mV, from -0.65 V vs. Fc (unmediated) to -1.07 V vs. Fc (mediated). They also saw increased selectivity for acetone (93%) under mediated conditions. Mechanistic studies indicate that the oxygen-based radical **Ar^{X}O** can abstract a H-atom from **Ir(H)(NH)**, facilitating the removal of one of the H-atoms bonded to the Ir metal center. They find that a second facile HAT reaction occurs from the PNP ligand with a second equivalent of **Ar^{X}O** radical, which results in the reformation of **IrN**. A large kinetic isotope effect (KIE = 4.2) was observed, which the authors attribute to the homolytic cleavage of the metal–hydride bond in the RDS of the reaction. They rule out a stepwise PT–ET mechanism as the initial PT would be initiated by P$_2$-Et deprotonating **Ir(H)(NH)**, which was experimentally ruled out even with base in excess. The stepwise ET–PT mechanism was also determined to be unlikely, as ET from **Ir(H)(NH)** to **Ar^{1}O** was calculated to be uphill by +9.7 kcal mol^{-1}; this is further supported by the large kinetic isotope effect observed which is in disagreement with the observation that a primary ($\sim$1) KIE is expected in rate-determining ET step mechanisms.[16,73] Thus, they reason the cycle is likely proceeding through a HAT from **Ir(H)(NH)** to **Ar^{X}O** rather than stepwise.

Discussion and conclusion

A successful strategy many have drawn from is electrifying thermal AOR systems or retrofitting electrocatalysts from other molecule transformations where metal hydrides form key intermediates. Both of these strategies provide easy entry-points for developing a molecular AOR electrocatalyst. From there, specific modifications can be made to better facilitate AOR, by developing ways to regenerate the starting complex electrochemically. Starting at the core of catalyst design, the first choice is that of the metal center. As the environmental impacts associated with precious metals has precipitated continued discussion, there has been significant interest surrounding developing first-row transition metal catalysts for the AOR.[8,14,25,27,35,43] Later transition metals, d^8–d^{10} are the most popular choices, since generating high-valent states with these compounds can produce powerful oxidants. The stability of the metal-center when highly oxidized is particular important when considering a system which may proceed through a metal-oxo intermediate. On the other hand, as many AOR mechanisms proceed through a metal-hydride intermediate, White and Waldie highlight the importance of thermodynamic hydricity ($\Delta G_{H^-}^{\circ}$) of the metal-hydride complex as an important parameter for identifying suitable catalysts.[27] When reconciled against the hydricity of substrate's C–H bond, the hydricity of the metal-hydride species can be used to determine if hydride transfer between metal and substrate is thermodynamically

favorable.[27] However, this parameter does not take into account the kinetic favorability of the hydride transfer reaction, which may be affected by factors such as the inner- or outer-sphere nature of the transfer.[75,76]

Moving outwards to the primary coordination sphere, the role of ligand framework in AOR should be considered next. Controlling catalyst speciation is crucial for eliminating side-phenomena to improve activity and stability. The presence of multiple labile ligands allows for more variable speciation. Such is the case for the **Ni(P$_2$N$_2$)** system, where there are up to four labile coordination sites available. Catalysis is initiated by the binding of a BnOH ligand, which is unfavorable, and also must compete with the binding of solvent and base.[25,29] **Ni(P$_2$N$_2$)(L)$_2$** is known to form a high-spin species where two additional L ligands coordinate to the metal center, eventually forming the stable six-coordinate **Ni(P$_2$N$_2$)(L)$_4$** species.[26,29] Under conditions for electrochemical AOR, this can lead to the formation of an off-cycle stable species **Ni(P$_2$N$_2$)(L)$_3$(BnOH)**, which inhibits turnover signficantly.[29] A similar pathway involving isomerization of **Fe(PNP)** and subsequent decomposition into an inert Fe^0 species has been attributed to deactivation in that system.[34]

Metal-oxo complexes, in general, are plagued by the formation of dimers. **Fe(TAML)**, **Ru(tpy)(bpy)**, and even the **Ru$_3$O** cluster all have reported examples of dimerization.[44,51,55,56,58,77] Dimerization may be the resting state of the catalytic cycle, like in **Fe(TAML)**, in which case one must consider how to shift equilibrium back on-cycle. Dimerization may also unlock some more interesting but complex electrochemical properties, like in the **Ru$_3$O** cluster.[56,77] Or it can simply indicate decomposition, which is the most significant outcome to avoid. A previous iteration of **Ru(tpy)(bpy)** using two bpy ligands, was prone to decomposition via dimer, but this was prevented by substituting in the tpy ligand.[55] Generally dimerization can be a result of dissociation of a ligand which then allows for the dimer to form. Therefore, this could possibly be avoided with the inclusion of more strongly bound ligands, or ones with additional denticity.

The AOR catalysts examined in this work all have at least one bi- or tridentate ligand, regardless of whether metal hydrides or oxos serve as intermediates. The rigidity of chelating ligands should be advantageous in controlling speciation and maintaining active site geometry. However, there must be at least one accessible coordination site for catalysis to proceed. Inclusion of a second **P$_2$N$_2$** ligand with the **Ni(P$_2$N$_2$)** catalyst was investigated, but this was shown inhibit catalysis for the AOR.[25] The pendent groups on the bulky **P$_2$N$_2$** framework likely block access to the active site, preventing the necessary substrate coordination.[26] As introduced above, recent work by Rodrigues et al. demonstrated the effect of additional chelating ligands on the **Cu/TEMPO** system. Modulating the amount of coordination sites through the inclusion of additional equivalents of bipyridine ligand increased the rate of co-catalysis observed by CV.[69] Since both the substrate and TEMPO must coordinate to the metal center, during the reaction, this suggests that a flexible tri- or tetradentate ligand for Cu might improve stability and

activity, without the added complexity of variable speciation at Cu.[14,64,65,69] Another viable strategy could be to pair a tridentate structural framework with an additional bidentate ligand, as in the **Ru(CNN)(dppb)** catalyst, where greater speciation control is observed.

Indeed, the use of four-coordinate planar ligands in other electrocatalyst systems are well studied, along with the benefits that secondary sphere modification can provide.[13] As introduced above, there are two examples using the four-coordinate **TAML** ligand framework to support Fe centers for electrochemical AOR. Since the reoxidation of the **Fe(TAML)** catalyst to the active oxo form occurs through PCET reactions, the strategy of pendent base inclusion on the ligand to improve reaction kinetics could reasonably applied to **Fe(TAML)** inspired by the example of the **Ni(P₂N₂)** complex. Indeed, the **Ir(PNP)** catalyst developed by Waymouth and co-workers, like the **Ni(P₂N₂)** complex, relies on ligand participation in proton transfer steps.[16,34,73] The **Co(P₃)** ligand framework does not directly participate in the catalytic cycle, lacking a suitably basic site for protonation by the relevant substrate pK_a values. While catalyst regeneration of **Co(P₃)** is facile, unlike **Ni(P₂N₂)**, the coordination of the alcohol is sluggish and TOF is low. As we suggest here, others have also proposed the idea of incorporating a more basic site onto the **P₃** ligand framework to improve TOF.[27]

Modification of the catalyst ligand framework with electron-withdrawing or electron-donating groups (EWG, EDG) is also a proven strategy to improving activity. Reducing the potential required to regenerate the active catalyst ($E_{1/2}$) is desirable, and can be accomplished through inclusion of EDG; but this can in turn decrease the Lewis acidity of the metal-center, and weaken substrate binding.[27] This can have conflicting impacts: shifting the **Ni**^{II/I} redox couple to more negative potentials leads to an increase in pendent amine basicity for **Ni(P₂N₂)₂** complexes in reactions with H₂.[78–80] In AOR systems, this change in basicity correlates to a ten-fold increase in rate of catalysis.[25] Thus, the effects of potential tuning must be balanced with corresponding changes in basicity in order to achieve the desired reactivity. For AOR systems where the binding of substrate is facile (and therefore not the RDS), a weakening of substrate coordination may not be significantly impactful on the rate, but the thermodynamic benefit from decreasing $E_{1/2}$ may be significant.

Finally, we reach the outer-coordination sphere parameters, including solvent and base choice. Work in the Waymouth group demonstrated the influence of base and solvent on activity and mechanism, which is general to many systems.[5,9,27] In the AOR systems examined here, **Ni(P₂N₂)**, **Co(P₃)**, and **Cu/TEMPO** all have a RDS involving unfavorable substrate coordination. It has been introduced above in discussion that base, solvent, and substrate can all compete for coordination in the presence of open coordination sites. NEt₃ is known to compete with BnOH for coordination in **Cu(bpy)**_n complexes.[69] **Ni(P₂N₂)** demonstrates a specific affinity to bind amines, including amine-substituted alcohols (*p*-NH₂)BnOH, which prevents catalytic turnover.[25,29] When using a more sterically hindered base (iPr₂EtN *vs.* NEt₃), **Ni(P₂N₂)** demonstrated an increased rate (*ca.* 3x) which

is thought to be due steric bulk preventing coordination to the metal-center.[25]

Speelman *et al.* have developed a universal method for reporting and calculating overpotential in organic systems.[31] The equilibrium potential for a catalytic reaction ($E^{\circ\prime}$) under non-standard conditions is related to the standard potential for the reaction E° by (1) solvent, (2) substrate, and (3) base.[31] Standard potential decreases ($E^{\circ\prime}$) as stronger bases are used (pK_a (HB⁺) increases). Assuming no significant change in E_{cat} for the PDS across bases, a stronger base should correlate to an increased overpotential. The bases used in the works presented here are all reasonably strong. Despite DFT studies with **Fe(PNP)** estimating a relatively mild pK_a of ∼12 for the metal-hydride, a base with a conjugate acid pK_a approximately 10 orders of magnitude weaker is required to drive this reaction.[34] This necessarily introduces a significant source of overpotential for electrocatalysis.[31] Ideally, further catalyst development to address kinetic limitations will eventually lead to conditions where strong bases are no longer required for catalysis. Besides the significant overpotentials created, strong bases often limit stability and lead to catalyst decomposition.[34,43]

Moving to an aqueous or neat alcohol solvent, the prevalence of the metal-oxo molecular catalysts dominates the number of metal-hydride catalysts. One exception being that **Ir(PNP)** and the **Ir/Ar^X O** co-catalytic system are both capable of AOR in neat IPA.[16] The availability of coordinating hydroxyl, hydroxide, and aquo ligands in the aqueous media will likely promote generation of oxygenated species. If you recall in Fig. 1, many of the intermediates require an addition of a hydroxyl radical (seen in red) to form, meaning those intermediate pathways are primarily relevant in aqueous catalyst systems. A benefit of being in an aqueous system is that it is possible to use milder bases, typically with well-defined buffer systems.[44,51,59,62]

The final outer-coordination sphere modification used is the inclusion of a redox mediator. Broadly, the inclusion of a redox mediator (RM) in a catalytic reaction can serve to improve the kinetics (k_{cat}) and/or the thermodynamics (E°) of the transformation. Here, we categorize the improvement of kinetics to be associated with facilitating the rate-determining step (RDS), while the improvement of thermodynamics to be associated with facilitating the potential-determining step (PDS). Although the reality is assuredly that the interplay between reaction kinetics and thermodynamics is not easily separable, for the sake of a categorical discussion this is the chosen paradigm.[74] When developing a co-catalytic system, having prior knowledge of how the catalyst operates is beneficial for selecting a RM capable of targeting the most sluggish and ineffective steps.[9] The decision to target the RDS or the PDS will depend on how the catalyst behaves under catalytic conditions. Another important element for the optimization of the co-catalytic conditions is the optimization of the relative concentrations of catalyst and RM. The interaction of catalyst and RM is always a pre-equilibrium step to the rate-limiting intermediates and transition states of the electrocatalytic cycle, which can be manipulated through deliberate alteration of concentrations or concentration ratios.[9,81] This means that co-catalytic increases

in activity should scale differently than single-component homogeneous systems.[9]

As of writing, there are only three published molecular co-catalytic systems for the electrocatalytic AOR. The first published system by Badalyan and Stahl demonstrates the cooperativity of **Cu(bpy)/TEMPO**. The two later co-catalytic systems, both published by the Waymouth group, follow similar mechanisms: the coordination of the substrate and subsequent product release are facile, but catalyst regeneration is a challenge. This is at odds with the unfavorable substrate coordination and product release observed for the **Cu/TEMPO** system. Thus, facilitating catalyst regeneration for the metal-hydride intermediate species observed by the Waymouth group would benefit from targeting the PDS step for optimization.

The comprehensive guidelines for RM selection developed by the Waymouth group are reiterated here, with slight modifications as to encompass systems without a metal-hydride intermediate:[9,15,16] (1) BDFE of any formed bonds should be similar, if not greater than, the BDFE of those broken, since thermodynamic driving force is a primary determinant in HAT reactivity.[9,82] (2) $E_{1/2}$ and pK_a of the RM should lie close to the thermodynamic potential for the AOR. (3) $E_{1/2}$ of RM should occur at a lower potential compared to E_{cat}. (4) pK_a of RM should not allow for protonation of any relevant metal hydride species. These criteria should hold true for targeting either the RDS or PDS of a catalyst system.

Structural trends for the AOR RMs are still emerging, but some general connections can be drawn. The non-transition metal-based RMs are stable, oxygen-based radical species, adjacent to a sterically protected ring structure. The **Ar^{X}O** mediators deemed suitable in the **Ir/Ar^{X}O** system all have alkyl groups (R = Me, *t*Bu) at the 2,6 positions, where radical character can localize through resonance. This matches the substitution pattern seen in TEMPO and TEMPO-derivates examined by Rafiee *et al.*, who determined that the thermodynamic driving force associated with a more positive RM $E_{1/2}$ plays a significant role at increasing rates, despite the anticipated trend of decreasing rate due to increasing steric hindrance.[20,66] Balancing the effects of RM structural modifications is tricky due to the complex interplay between pK_a, $E_{1/2}$, and BDFE.[16,74] Inclusion of EDG can increase pK_a while lowering $E_{1/2}$, but in turn will decrease BDFE; and *vice versa*. Finding a balance between these three parameters is crucial when considering structural modification of a redox mediator. Individual modifications of the RM must then be undertaken with the goal of better alignment with the pK_a and $E_{1/2}$ of the catalyst. The ability to independently tune system reactivity without altering the catalyst is attractive for helping to define and maintain clear structure-function trends.[9]

McLoughlin *et al.* opted to select a Ru-based transition-metal RM because the thermodynamic and kinetic properties of transition-metal complexes easy to tune through synthetic modification.[15] Recently, structural modifications of the [Ru(acac)$_2$-(pyimN)] framework were found to be capable of "decoupling" the relationship between $E_{1/2}$ and pK_a typically observed.[83] This is an exciting prospect for both catalyst design and RM design as it allows for the freedom of adjusting one parameter with minimal impact on the other, potentially aiding in breaking molecular scaling relationships.[83,84] Despite these initial reports demonstrating great success—inclusion of RMs can cause significant reduction in operating potential (up to 0.5 V) alongside a reported increase in TOF (up to 5x!)—and establishing clear guidelines for the development of co-catalytic systems, there have been no new co-catalytic systems published for the AOR since 2020;[14–16,31] this is an area ripe for new advancements![9,27]

All of the properties of the electrocatalyst system are selected with the desire to maximize rates (TOF) while minimizing overpotential (η).[84] Such is the foundation of the molecular scaling relationship, where the improvement of one parameter is expected to come at a detriment to the other. Circumventing the rate–overpotential relationship can be achieved through mechanistic understanding which in turn guides system-level control.[78] Indeed, studies with the **Ni(P$_2$N$_2$)** type complexes for HER clearly demonstrate that catalyst electronics and structural dynamics can be leveraged both individually and in combination to access different regions of the rate–overpotential relationship.[78]

Rather than focusing on "breaking" the scaling relationship, Mayer and co-workers have emphasized that combining scaling relationships can improve catalyst properties beyond what individual tuning of a single parameter can achieve.[84] Molecular electrocatalysts follow multiple scaling relationships, both kinetic and thermodynamic. In line with Mayer's philosophy, these intricate relationships between pK_a, $E_{1/2}$, electron density, and BDFE in molecular catalysis can be viewed as tuning controls for the system.[74,78,84] Inclusion of a RM can further aid in tuning a system, as the inclusion of a RM can bypass the molecular scaling relationships, allowing us access to a region of high TOF, low η catalysis for the AOR.[9,13]

As the scope of AOR continues to advance, it is hoped that more progress will be made towards achieving catalysis with MeOH as a substrate. While the 2H$^+$/2e$^-$ oxidation from MeOH to PhCHO would likely be the easiest transformation to target, the 6H$^+$/6e$^-$ complete oxidation to CO$_2$ is necessary for ultimate implementation into a DMFC. Of the examples discussed in this work, only the **Cu/TEMPO** and **Ru$_3$O** systems have displayed any catalytic activity with MeOH as the substrate. There are examples of thermal catalysts capable of the 6H$^+$/6e$^-$ transformation, which have been discussed in other works,[6] but there has yet to be a homogeneous electrocatalyst capable of the complete oxidation to CO$_2$. It should be reiterated that the catalyst systems highlighted here were all adapted from related thermal systems or similar electrochemical transformations. Drawing inspiration from well-studied thermal catalyst systems capable of the desired reaction seems to be one of the most promising avenues for advancement towards the ultimate goal of efficient and selective MeOH oxidation.

Author contributions

M. C. M. and C. W. M. wrote the manuscript. C. W. M. supervised the writing.

Data availability

No primary research results, software or code have been included and no new data were generated or analysed as part of this review.

Conflicts of interest

There are no conflicts to declare.

Acknowledgements

Notes and references

1 U.S. Energy System Factsheet, https://css.umich.edu/publications/factsheets/energy/us-energy-system-factsheet, (accessed September 2024).
2 U.S. Energy Facts Explained, https://www.eia.gov/energyexplained/us-energy-facts/, (accessed September 2024).
3 C. Tang, Y. Zheng, M. Jaroniec and S. Qiao, Angew. Chem., Int. Ed, 2021, 60, 19572.
4 M. Deitermann, Z. Huang, S. Lechler, M. Merko and M. Muhler, Chem. Ing. Tech., 2022, 94, 1573.
5 A. W. Cook and K. M. Waldie, ACS Appl. Energy Mater., 2020, 3, 38.
6 E. Alberico and M. Nielsen, Chem. Commun., 2015, 51, 6714.
7 M. Singh, H. M. Sharma, J. Kaur, D. K. Das, M. Ubaidullah, R. K. Gupta and A. Kumar, Mol. Catal., 2024, 557, 113982.
8 A. Yuda, A. Ashok and A. Kumar, Catal. Rev., 2022, 64, 126.
9 A. G. Reid and C. W. Machan, J. Am. Chem. Soc., 2023, 145, 2013.
10 S. Sahoo, E. K. Johnson, X. Wei, S. Zhang and C. W. Machan, Energy Adv., 2024, 3, 2280.
11 E. K. Johnson, D. P. Musikanth, C. K. Webber, T. B. Gunnoe, S. Zhang and C. W. Machan, J. Am. Chem. Soc., 2025, 147, 10459.
12 M. Beygisangchin, S. K. Kamarudin, S. A. Rashid, N. A. I. Md Ishak, N. A. Karim, J. Jakmunee, I. Letchumanan, I. H. Hanapi, S. H. Osman and A. H. Baghdadi, J. Environ. Chem. Eng., 2024, 12, 114447.
13 M. E. Moberg and C. W. Machan, Acc. Chem. Res., 2024, 57, 2326.
14 A. Badalyan and S. S. Stahl, Nature, 2016, 535, 406.
15 E. A. McLoughlin, K. C. Armstrong and R. M. Waymouth, ACS Catal., 2020, 10, 11654.
16 C. M. Galvin and R. M. Waymouth, J. Am. Chem. Soc., 2020, 142, 19368.
17 R. Ciriminna, G. Palmisano and M. Pagliaro, ChemCatChem, 2015, 7, 552.
18 R. Ciriminna, M. Ghahremani, B. Karimi and M. Pagliaro, ChemistryOpen, 2017, 6, 5.
19 C. W. Anson and S. S. Stahl, Chem. Rev., 2020, 120, 3749.
20 J. E. Nutting, M. Rafiee and S. S. Stahl, Chem. Rev., 2018, 118, 4834.
21 C. Yang, S. Arora, M. Maldonado, D. A. Pratt and C. R. J. Stephenson, Nat. Rev. Chem., 2023, 7, 653.
22 D. Leifert and A. Studer, Chem. Rev., 2023, 123, 10302.
23 J. B. Gerken and S. S. Stahl, ACS Cent. Sci., 2015, 1, 234.
24 Z. Ma, K. T. Mahmudov, V. A. Aliyeva, A. V. Gurbanov and A. J. L. Pombeiro, Coord. Chem. Rev., 2020, 423, 213482.
25 C. J. Weiss, P. Das, D. L. Miller, M. L. Helm and A. M. Appel, ACS Catal., 2014, 4, 2951.
26 E. S. Wiedner, J. Y. Yang, W. G. Dougherty, W. S. Kassel, R. M. Bullock, M. R. DuBois and D. L. DuBois, Organometallics, 2010, 29, 5390.
27 N. M. White and K. M. Waldie, Dalton Trans., 2024, 53, 11644.
28 C. J. Weiss, E. S. Wiedner, J. A. S. Roberts and A. M. Appel, Chem. Commun., 2015, 51, 6172.
29 T. Gunasekara, Y. Tong, A. L. Speelman, J. D. Erickson, A. M. Appel, M. B. Hall and E. S. Wiedner, ACS Catal., 2022, 12, 2729.
30 It should be acknowledged that the conceptualization of a single "rate-determining" step for a catalytic process is an oversimplification; rather, there is both a rate-determining intermediate and a rate-determining transition state, which may or may not be related to a single chemical step. Interested readers are directed to the following articles for more information on the idea of rate-determining states and a discussion on the interplay between computational and experimental electrochemistry: S. Kozuch and S. Shaik, Acc. Chem. Res., 2011, 44, 101; G. Durin and C. Costentin, ACS Catal., 2025, 15, 2504.
31 A. L. Speelman, J. B. Gerken, S. P. Heins, E. S. Wiedner, S. S. Stahl and A. M. Appel, Energy Environ. Sci., 2022, 15, 4015.
32 L. E. Fernandez, S. Horvath and S. Hammes-Schiffer, J. Phys. Chem. C, 2012, 116, 3171.
33 S. Horvath, L. E. Fernandez, A. V. Soudackov and S. Hammes-Schiffer, Proc. Natl. Acad. Sci. U. S. A., 2012, 109, 15663.
34 E. A. McLoughlin, B. D. Matson, R. Sarangi and R. M. Waymouth, Inorg. Chem., 2020, 59, 1453.
35 K. M. Waldie, K. R. Flajslik, E. McLoughlin, C. E. D. Chidsey and R. M. Waymouth, J. Am. Chem. Soc., 2017, 139, 738.
36 M. Trincado, J. Bösken and H. Grützmacher, Coord. Chem. Rev., 2021, 443, 213967.
37 M. Bellini, M. Bevilacqua, J. Filippi, A. Lavacchi, A. Marchionni, H. A. Miller, W. Oberhauser, F. Vizza, S. P. Annen and H. Grützmacher, ChemSusChem, 2014, 7, 2432.
38 K. R. Brownell, C. C. L. McCrory, C. E. D. Chidsey, R. H. Perry, R. N. Zare and R. M. Waymouth, J. Am. Chem. Soc., 2013, 135, 14299.
39 E. A. Bielinski, P. O. Lagaditis, Y. Zhang, B. Q. Mercado, C. Würtele, W. H. Bernskoetter, N. Hazari and S. Schneider, J. Am. Chem. Soc., 2014, 136, 10234.
40 S. Chakraborty, P. O. Lagaditis, M. Förster, E. A. Bielinski, N. Hazari, M. C. Holthausen, W. D. Jones and S. Schneider, ACS Catal., 2014, 4, 3994.
41 H. Jiao, K. Junge, E. Alberico and M. Beller, J. Comput. Chem., 2016, 37, 168.
42 C. Costentin, S. Drouet, M. Robert and J.-M. Savéant, J. Am. Chem. Soc., 2012, 134, 11235.
43 S. P. Heins, P. E. Schneider, A. L. Speelman, S. Hammes-Schiffer and A. M. Appel, ACS Catal., 2021, 11, 6384.
44 A. Das, J. E. Nutting and S. S. Stahl, Chem. Sci., 2019, 10, 7542.
45 A. Gunay and K. H. Theopold, Chem. Rev., 2010, 110, 1060.
46 A. S. Borovik, Chem. Soc. Rev., 2011, 40, 1870.
47 Z. Chen and G. Yin, Chem. Soc. Rev., 2015, 44, 1083.
48 K.-B. Cho, H. Hirao, S. Shaik and W. Nam, Chem. Soc. Rev., 2016, 45, 1197.
49 T. J. Collins and A. D. Ryabov, Chem. Rev., 2017, 117, 9140.
50 E. L. Demeter, S. L. Hilburg, N. R. Washburn, T. J. Collins and J. R. Kitchin, J. Am. Chem. Soc., 2014, 136, 5603.
51 H. Kuiry, D. Das, S. Das, S. Chakraborty, B. Chandra and S. S. Gupta, Faraday Discuss., 2022, 234, 42.
52 N. Von Wolff, O. Rivada-Wheelaghan and D. Tocqueville, ChemElectroChem, 2021, 8, 4019.
53 E. L. Lebeau, R. A. Binstead and T. J. Meyer, J. Am. Chem. Soc., 2001, 123, 10535.
54 M. S. Thompson and T. J. Meyer, J. Am. Chem. Soc., 1982, 104, 4106.
55 B. A. Moyer, M. S. Thompson and T. J. Meyer, J. Am. Chem. Soc., 1980, 102, 2310.
56 H. Toma, Coord. Chem. Rev., 2001, 219–221, 187.
57 J. A. Baumann, D. J. Salmon, S. T. Wilson, T. J. Meyer and W. E. Hatfield, Inorg. Chem., 1978, 17, 3342.
58 J. A. Baumann, D. J. Salmon, S. T. Wilson and T. J. Meyer, Inorg. Chem., 1979, 18, 2472.
59 H. E. Toma, K. Araki, A. L. B. Formiga, A. D. P. Alexiou and G. S. Nunes, Quím. Nova, 2010, 33, 2046.
60 S. Romain, L. Vigara and A. Llobet, Acc. Chem. Res., 2009, 42, 1944.
61 A. E. Pérez Mendoza, N. Naidek, E. C. Cesca, J. C. Sagás, E. S. Orth, A. J. G. Zarbin and H. Winnischofer, ACS Appl. Nano Mater., 2020, 3, 6757.
62 G. S. Nunes, A. D. P. Alexiou, K. Araki, A. L. B. Formiga, R. C. Rocha and H. E. Toma, Eur. J. Inorg. Chem., 2006, 1487.
63 J. M. Hoover, B. L. Ryland and S. S. Stahl, J. Am. Chem. Soc., 2013, 135, 2357.
64 B. L. Ryland, S. D. McCann, T. C. Brunold and S. S. Stahl, J. Am. Chem. Soc., 2014, 136, 12166.
65 B. L. Ryland and S. S. Stahl, Angew. Chem., Int. Ed., 2014, 53, 8824.
66 M. Rafiee, K. C. Miles and S. S. Stahl, J. Am. Chem. Soc., 2015, 137, 14751.

67 A. Mishra, J. Kim, M. Zorigt, A. I. B. Romo, R. Gaddam, J. E. Braun, D. Ziviani and J. Rodríguez-López, *ACS Sustainable Chem. Eng.*, 2023, **11**, 6241.

68 M. F. Semmelhack, C. S. Chou and D. A. Cortes, *J. Am. Chem. Soc.*, 1983, **105**, 4492.

69 M. G. B. Rodrigues, A. L. P. De Melo, M. D. Coutinho-Neto and C. A. Angelucci, *ChemCatChem*, 2024, e202401444.

70 M. Bourrez, R. Steinmetz, S. Ott, F. Gloaguen and L. Hammarström, *Nat. Chem.*, 2015, **7**, 140.

71 A. Wu, J. Masland, R. D. Swartz, W. Kaminsky and J. M. Mayer, *Inorg. Chem.*, 2007, **46**, 11190.

72 A. Friedrich, R. Ghosh, R. Kolb, E. Herdtweck and S. Schneider, *Organometallics*, 2009, **28**, 708.

73 Z. E. Clarke, P. T. Maragh, T. P. Dasgupta, D. G. Gusev, A. J. Lough and K. Abdur-Rashid, *Organometallics*, 2006, **25**, 4113.

74 R. G. Agarwal, S. C. Coste, B. D. Groff, A. M. Heuer, H. Noh, G. A. Parada, C. F. Wise, E. M. Nichols, J. J. Warren and J. M. Mayer, *Chem. Rev.*, 2022, **122**, 1.

75 M. R. Espinosa, M. Z. Ertem, M. Barakat, Q. J. Bruch, A. P. Deziel, M. R. Elsby, F. Hasanayn, N. Hazari, A. J. M. Miller, M. V. Pecoraro, A. M. Smith and N. E. Smith, *J. Am. Chem. Soc.*, 2022, **144**, 17939.

76 K. R. Brereton, N. E. Smith, N. Hazari and A. J. Miller, *Chem. Soc. Rev.*, 2020, **49**, 7929.

77 C. P. Kubiak, *Inorg. Chem.*, 2013, **52**, 5663.

78 C. M. Klug, A. J. P. Cardenas, R. M. Bullock, M. O'Hagan and E. S. Wiedner, *ACS Catal.*, 2018, **8**, 3286.

79 S. Chen, M.-H. Ho, R. M. Bullock, D. L. DuBois, M. Dupuis, R. Rousseau and S. Raugei, *ACS Catal.*, 2014, **4**, 229.

80 E. S. Wiedner, A. M. Appel, S. Raugei, W. J. Shaw and R. M. Bullock, *Chem. Rev.*, 2022, **122**, 12427.

81 C. Costentin and J. Savéant, *ChemElectroChem*, 2014, **1**, 1226.

82 C. T. Saouma and J. M. Mayer, *Chem. Sci.*, 2014, **5**, 21.

83 B. D. Groff, M. Cattaneo, S. C. Coste, C. A. Pressley, B. Q. Mercado and J. M. Mayer, *Inorg. Chem.*, 2023, **62**, 10031.

84 D. J. Martin, B. Q. Mercado and J. M. Mayer, *Sci. Adv.*, 2020, **6**, eaaz3318.